



Discovery and optimization of a potent and selective triazolopyridinone series of c-Met inhibitors

Christiane M. Bode^{a,*}, Alessandro A. Boezio^{a,*}, Brian K. Albrecht^a, Steven F. Bellon^a, Loren Berry^a, Martin A. Broome^b, Deborah Choquette^a, Isabelle Dussault^b, Richard T. Lewis^a, Min-Hwa Jasmine Lin^a, Karen Rex^b, Douglas A. Whittington^a, Yajing Yang^b, Jean-Christophe Harmange^a

^a Amgen Inc., 360 Binney St., Cambridge, MA 02142, USA

^b Amgen Inc., One Amgen Center Drive, Thousand Oaks, CA 91320, USA

ARTICLE INFO

Article history:

Received 3 February 2012

Revised 12 April 2012

Accepted 16 April 2012

Available online 25 April 2012

Keywords:

Tyrosine kinase

c-Met

Triazolopyridinones

ABSTRACT

Deregulation of the receptor tyrosine kinase c-Met has been implicated in several human cancers and is an attractive target for small molecule drug discovery. Herein, we report the discovery of a structurally diverse series of carbon-linked quinoline triazolopyridinones, which demonstrates nanomolar inhibition of c-Met kinase activity. This novel series of inhibitors exhibits favorable pharmacokinetics as well as potent inhibition of HGF-mediated c-Met phosphorylation in a mouse liver pharmacodynamic model.

© 2012 Elsevier Ltd. All rights reserved.

The receptor tyrosine kinase c-Met and its endogenous ligand, hepatocyte growth factor (HGF), are implicated in several cellular processes relevant to cancer, including cell proliferation, cell migration, and invasive growth. They also play an important role in embryonic development and wound healing.¹ However, deregulation of the c-Met/HGF pathway can lead to tumorigenesis and metastasis.² Amplification of the MET gene, overexpression of c-Met and/or HGF, and constitutive activation conferred by sequence mutations are some of the mechanisms of deregulation which have been found in human cancers.³

There are several approaches to inhibiting the HGF/c-Met pathway currently being tested in the clinic.⁴ The appeal of an ATP-competitive, small molecule inhibitor acting via the intracellular kinase domain is its potential to block both ligand-dependent and ligand independent activity of c-Met.⁵ We previously reported the discovery of a potent, orally active c-Met inhibitor for the treatment of cancer,⁶ and more recently disclosed two series of oxygen- and nitrogen-linked triazolopyridazines (**1** and **2**) as potent and selective c-Met inhibitors (Fig. 1).^{7,8} However, these compounds displayed poor overall solubility and exhibited short duration of coverage in our pharmacodynamic model. In efforts to improve these limitations, further exploration of these structural chemotypes led to the discovery of a triazolopyridinone series of c-Met inhibitors (**3**) that are highly potent and selective. Herein, we

describe the design, synthesis and improved in vivo efficacy for this class of compounds.

Based on the evolution of the O- and N-linked triazolopyridazine series (**1** and **2**), we hypothesized that intramolecular hydrogen bonds between the oxygen or nitrogen tether and the quinoline or naphthyridine moiety were important for maintaining a favorable binding conformation, and hence, enzyme and cellular potencies. Analysis of the co-crystal structure of **2** with c-Met showed that the inhibitor adopts a U-shaped conformation enveloping Met1211, and the 4-aminonaphthyridine makes key hydro-

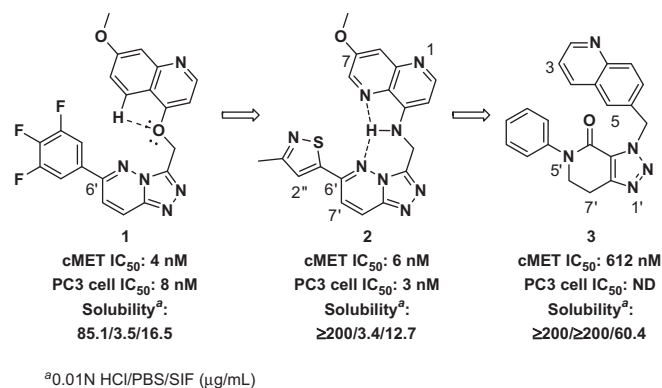


Figure 1. Core modifications that lead to the triazolopyridinone chemotype.⁹

* Corresponding authors. Tel.: +1 617 444 5104; fax: +1 617 621 3907.

E-mail address: aboenzio@amgen.com (A.A. Boezio).

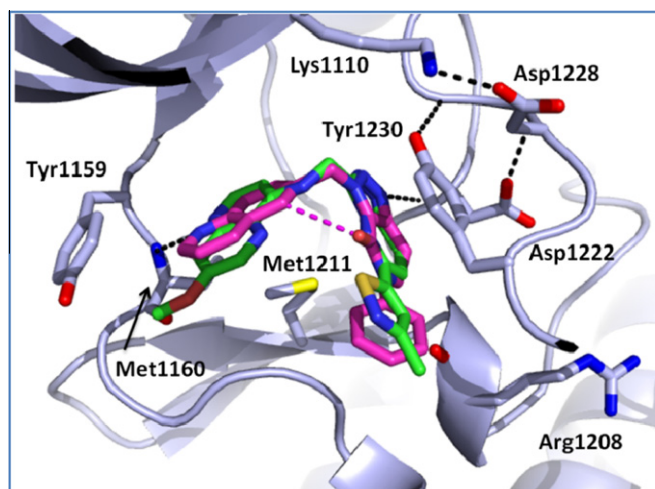


Figure 2. Crystal structure overlay of c-Met + **2** (green) and **3** (pink).

gen bond interactions with linker residue Met1160 (Fig. 2, green structure). In the design of a new scaffold, we hypothesized that the 4-aminonaphthridine of compound **2** could be replaced with a carbon-linked quinoline (**3**), as the quinoline nitrogen should reside in approximately the same position for interaction with Met1160. However, this change could disrupt the U-shaped conformation enforced by the intramolecular hydrogen bonds present in **1** and **2**. In order to maintain that structural feature in the new scaffold and to introduce non-planar elements that could improve solubility,¹⁰ the triazolopyridazine core was modified to a dihydro-triazolopyridinone. This placement of atoms may allow the carbonyl to favorably interact with the proton at the C-5 position of the quinoline,¹¹ and the saturation across C-6' and C-7' could disrupt the packing of the crystal lattice. Based on this hypothesis, the parent compound **3** (Fig. 1) with a phenyl group in the N-5' position was synthesized¹² and although a loss of enzyme potency was observed, this new core exhibited greater solubility than **1**

and **2**, and therefore provided a good starting point for lead optimization.

A co-crystal structure of **3** within the catalytic domain of unphosphorylated c-Met was obtained (overlaid with **2** in Fig. 2),¹³ indicating that the inhibitor adopted the desired U-shaped binding mode around Met1211. A favorable intramolecular interaction was also observed between the carbonyl oxygen and the C-5 hydrogen of the quinoline (3.2 Å). The quinoline nitrogen atom participates in a single-point hydrogen bond with linker residue Met1160, while N-1' of the dihydro-triazolopyridinone interacts with the backbone –NH of Asp 1222. In addition, a face-to-face π -stacking interaction is observed between the triazolopyridinone and Tyr1230.

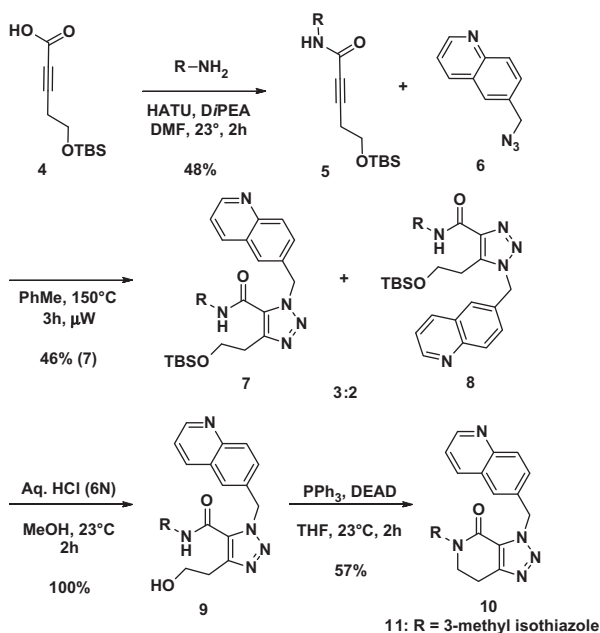
Having identified a structurally unique scaffold, our focus shifted to improving the c-Met potency of **3**. The SAR developed in our previously reported triazolopyridazine series indicated that variation of the C-6' substituent of **1** and **2** significantly impacted potency in both enzymatic and cellular assays. Accordingly, a synthetic route was developed that enabled rapid analoging at the corresponding N-5' position of **3** (Scheme 1). HATU amide coupling between the alkynyl acid **4** and the desired N-5' amine provided intermediate **5**. Dipolar cycloaddition of **5** with 6-(azidomethyl)quinoline (**6**) led to a 3:2 product ratio as observed by LC/MS, favoring the desired regioisomer **7**. After removing the silyl group, Mitsunobu cyclization yielded the substituted dihydro-triazolopyridinones **10**.¹⁴

Consistent with SAR established in the O- and N-linked triazolopyridazine series, a dramatic increase in enzyme potency was observed upon replacement of the phenyl group of **3** with 3-methyl isothiazole (**11**, 612 nM to 21 nM), and a cellular potency of 62 nM was also achieved. A positive interaction between the sulfur of the isothiazole and the oxygen from the dihydro-triazolopyridinone¹⁵ may favor a coplanar orientation of the N-5' substituent, resulting in optimal binding to c-Met.

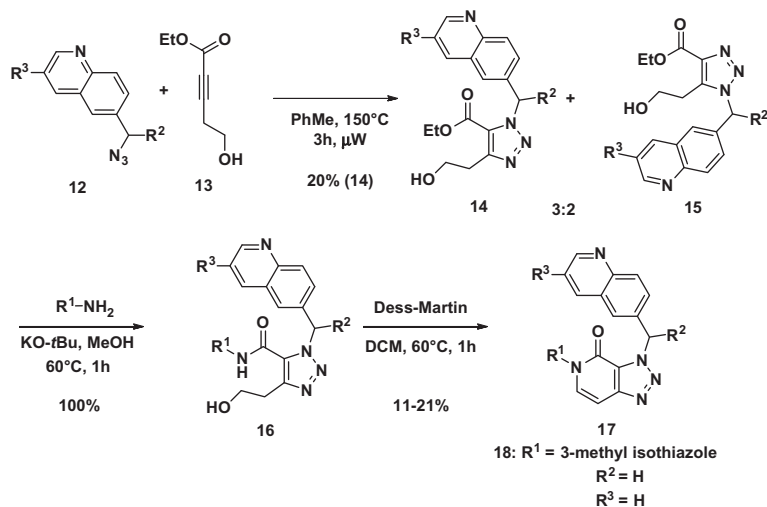
In the case of compound **2**, a two-point interaction was observed between the hydrogens appended at C-7' and C-2'' and the lone pairs of the carbonyl of Arg1208, as well as a face-to-face π -stacking interaction with the triazolopyridazine core and Tyr1230 (Fig. 2). The saturation in the dihydro-triazolopyridinone core at the C-6' and C-7' positions, incorporated to improve solubility, precluded **3** and **11** from fully engaging these interactions. Introducing unsaturation at this position to afford triazolopyridinone **18** increased the enzymatic and cellular potencies to 3 and 5 nM, respectively.¹⁶

The unsaturation of the triazolopyridinone core was introduced at a later stage in the synthesis, utilizing the same common intermediate leading to either the saturated or unsaturated molecule. The synthesis began with cycloaddition of the azidomethyl-quinoline **12** with ethyl-5-hydroxypent-2-ynoate (**13**) yielding the regioisomeric triazoles **14** and **15** (3:2). Compound **14** was then converted to the desired amide **16** (introducing the N-5' substitution), which upon exposure to Dess-Martin periodinane triggered an imine/enamine cyclization to yield the desired triazolopyridinones **17** (Scheme 2).

Although the introduction of the methyl isothiazole (compound **11**) and the unsaturated core (compound **18**) imparted enhanced potency in comparison to **3**, both changes led to a dramatic decrease in solubility (**11**: 43.2/2.2/<1 and **18**: 80.1/<1/4.8).¹⁷ Further modifications were made to address this issue. An overlay of the crystal structures of **2** and **3** (Fig. 2) indicates that substitution with a methoxy group at the 3-position of the quinoline in compound **3** could occupy the same solvent front as the methoxy group in compound **2**. Modification of this moiety could potentially increase solubility and potency, as was observed in the N-linked triazolopyridazine series. Addition of the ethoxymethoxy group in compound **20** (c-Met = 1 nM, PC3 cell = 2 nM) provided a slight



Scheme 1. Synthesis of dihydro-triazolopyridinones.



Scheme 2. Convergent synthesis of triazolopyridinones.

Table 1
Representative triazolopyridinones

Compd.	R ¹	R ²	R ³	cMET IC ₅₀ ^a (nM)	PC3 IC ₅₀ ^b (nM)
18		H	H	3	5
19		H	OMe	3	3
20		H	OCH ₂ CH ₂ OMe	1	2
21		Me	H	2	3
22		Me	OMe	1	2
23		Me	OCH ₂ CH ₂ OMe	1	2
24		H	OCH ₂ CH ₂ OMe	10	102
25		Me	OCH ₂ CH ₂ OMe	2	12
26		Me	H	7	17
27		Me	H	7	39
28		Me	H	3	37
29		H	OMe	12	110
30		H	OCH ₂ CH ₂ OMe	8	14
31		Me	OCH ₂ CH ₂ OMe	1	3
32		Me	OCH ₂ CH ₂ OMe	2	3

^a $n \geq 2$, inhibition of kinase activity in a biochemical assay.^b $n \geq 2$, inhibition of HGF-mediated c-Met phosphorylation in PC3 cells.

improvement in potency; however, the solubility was not greatly affected. (13.7/2.5/9.8).

Additionally, a methyl group was introduced at the methylene bridge in order to improve solubility by integrating another non-planar element as well as to maintain/increase potency by favoring the desired rotameric disposition of the two ring systems. We observed that the *S* enantiomer exhibited better potency than its *R* counterpart (**21**): (*S*) c-Met = 2 nM, PC3 cell = 3 nM versus (*R*)

c-Met = 42 nM, PC3 cell = 29 nM).¹⁸ Compound **21** also showed improved solubility compared to **18** ($\geq 200/4.5/22.4$).

To further explore the SAR of compounds **18–21**, a variety of heterocycles¹⁹ and fluorinated aromatic rings²⁰ at the R¹ position were synthesized. Table 1 illustrates the biochemical and cellular potencies of these compounds against c-Met. All of the R¹ substituents were tolerated when paired with the chiral (*S*)-methyl (R²) and/or the ether groups (R³). A more noticeable improvement in potency was observed when incorporating an (*S*)-methyl substituent at R² (**24** versus **25**, and **30** versus **31**). Compounds **29** and **30** indicated that the ethoxymethoxy substituent in the R³ position provided a slightly more cell-potent compound than the smaller methoxy group. Upon combining the best R² and R³ substituents, the fluorinated aromatic compound **32**, along with the 3-methyl isothiazole derivative **23**, were highlighted as R¹-diverse compounds with superior solubility profiles compared to **1** and **2** (**23**: 37.0/8.7/39.7; **32**: 127.7/11.1/37.7).

The metabolic stability and pharmacokinetic properties of **23** and **32** were evaluated (Table 2). For both compounds, moderate intrinsic clearance was observed across species. The plasma protein binding was greater than 95% in rat, mouse and human. Consistent with its turnover in rat liver microsomes, compound **32** showed a slightly higher in vivo clearance than **23**, resulting in a shorter half-life since both the volume of distribution and PPB were comparable for the compounds. The oral bioavailability of **23** was also higher than that of **32**.

Crystallographic analysis of **23** confirmed many of the structural design aspects we had incorporated throughout the optimization process, as well as those previously observed with **3** (Fig. 3).²¹ The two-point binding with the triazolopyridinone ring and the carbonyl of Arg1208 was restored, and more efficient π -stacking with Tyr1230 was observed. We also confirmed that the (*S*)-enantiomer of the chiral methyl group was preferred by the protein²² and this methyl substituent fills a small, lipophilic pocket in c-Met, defined by the side chains of Val1092, Leu1157, Ala 1226, and Lys1110.

Before assessing the in vivo pharmacological activity of our new series, compound **23** was screened for inhibitory activity against a broad panel of 100 kinases (Ambit screen), and displayed good overall selectivity against a range of tyrosine and serine/threonine kinases.²³

To demonstrate that compound **23** inhibits c-Met activity in vivo over time, a pharmacodynamic assay measuring changes in HGF-induced phosphorylation of c-Met in the mouse liver was

Table 2
In vitro ADME and in vivo PK properties of selected compounds

	23	32
RLM Cl ^a (μL/min/mg)	89	105
MLM Cl ^a (μL/min/mg)	68	98
HLM Cl ^a (μL/min/mg)	84	120
PPB ^b (%) Rat	98.2	98.0
Mouse	97.3	95.6
Human	98.8	95.5
<i>Rat pharmacokinetics</i> ^c		
Cl ^d (L/h/kg)	0.559	1.13
V _{ss} ^d (L/Kg)	2.53	2.38
T _{1/2} ^d (h)	3.40	1.81
AUC _{0→∞} ^e (ng h/mL)	1560	638
F ^e (%)	43	36

^a In vitro (RLM = rat liver microsomes; MLM = mouse liver microsomes; HLM = human liver microsomes).

^b Separation method = equilibrium dialysis.

^c In vivo experiments with male Sprague–Dawley rats (n = 3).

^d IV, 0.25 mg/kg (DMSO).

^e PO, 2 mg/kg (2% HPMC, 1% Tween 80 in H₂O, pH 2.2 w/MSA).

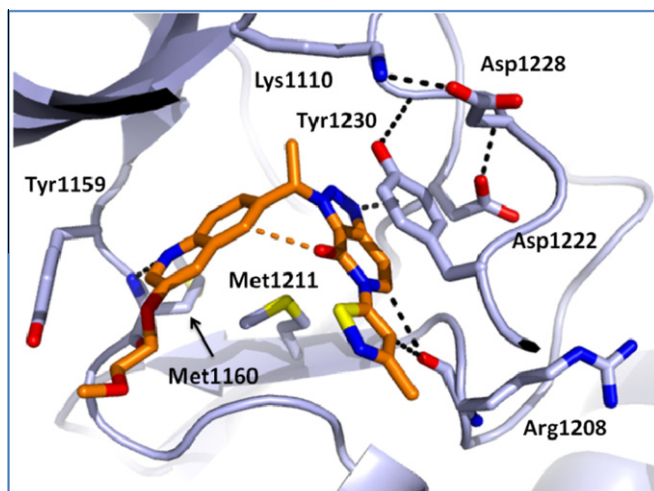


Figure 3. Crystal structure of c-Met + 23.

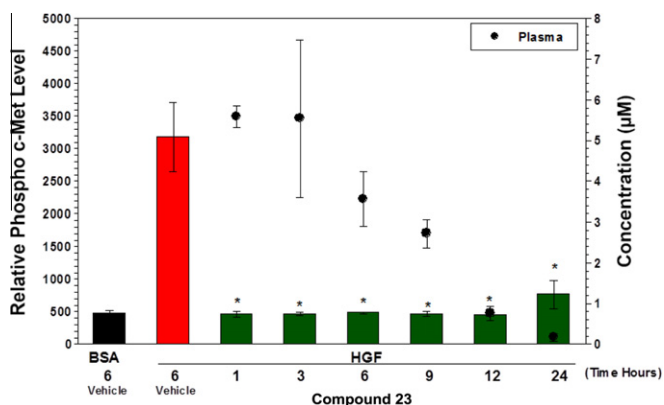


Figure 4. Compound 23 inhibits HGF-mediated c-Met phosphorylation in mouse liver when dosed at 10 mg/kg.²⁶

used (Fig. 4).²⁴ Mice were administered a single oral dose of compound 23 at 10 mg/kg. Human recombinant HGF was injected intravenously at 1, 3, 6, 9, 12 or 24 h post-dose. Liver and blood were harvested 5 min after administration of recombinant HGF.

c-Met phosphorylation was inhibited at least 89% through 24 h with an associated plasma concentration of less than 0.2 μM,²⁵ a much-improved result upon comparison to compounds 1 and 2, both of which showed inhibition >90% only up to 6 h, with a larger dose of 30 mg/kg.^{7,8}

In conclusion, through the use of structure-based design, a novel series of triazolopyridinone c-Met inhibitors was developed. The inhibitors, which incorporate key design elements present in compounds 1 and 2, potentially block the kinase activity of c-Met in both biochemical and cellular assays at a single-digit nanomolar level. Compound 23, which displayed a modest solubility improvement in relation to the progenitor series, exhibits an improved pharmacodynamic profile, significantly inhibiting HGF-mediated c-Met phosphorylation for up to 24 h in a mouse liver PD model.

Acknowledgments

Special thanks to both Roman Shimanovich and Kavita Shah for in vivo formulation support and to Earl Moore for analytical support of the PK and PD samples.

References and notes

- Giordano, S.; Ponzetto, C.; Di Renzo, M. F.; Cooper, C. S.; Comoglio, P. M. *Nature* **1989**, *339*, 155.
- Birchmeier, C.; Birchmeier, W.; Gherardi, E.; Vande Woude, G. F. *Nat. Rev. Mol. Cell Biol.* **2003**, *4*, 915.
- Dharmawardana, P. G.; Giubellino, A.; Bottaro, D. P. *Curr. Mol. Med.* **2004**, *4*, 855.
- Small molecules: (a) Cui, J. J. *Expert Opin. Ther. Patents* **2007**, *17*, 1035; Biologicals: (b) Cao, B.; Su, Y.; Oskarsson, M.; Zhao, P.; Kort, E. J.; Fisher, R. J.; Wang, L. M.; Vande Woude, G. F. *Proc. Natl. Acad. Sci. U.S.A.* **2001**, *98*, 7443.
- Porter, John *Expert Opin. Ther. Patents* **2010**, *20*, 159.
- Liu, L.; Siegmund, A.; Xi, N.; Kaplan-Lefko, P.; Rex, K.; Chen, A.; Lin, J.; Moriguchi, J.; Berry, L.; Huang, L.; Teffera, Y.; Yang, Y.; Zhang, Y.; Bellon, S. F.; Lee, M.; Shimanovich, R.; Bak, A.; Dominguez, C.; Norman, M. H.; Harmange, J.-C.; Dussault, I.; Kim, T.-S. *J. Med. Chem.* **2008**, *51*, 3688.
- Albrecht, B. K.; Harmange, J.-C.; Bauer, D.; Berry, L.; Bode, C.; Boezio, A. A.; Chen, A.; Choquette, D.; Dussault, I.; Fridrich, C.; Hirai, S.; Hoffman, D.; Larrow, J. F.; Kaplan-Lefko, P.; Lin, J.; Lohman, J.; Long, A. M.; Moriguchi, J.; O'Connor, A.; Potashman, M. H.; Reese, M.; Rex, K.; Siegmund, A.; Shah, K.; Shimanovich, R.; Springer, S. K.; Teffera, Y.; Yang, Y.; Zhang, Y.; Bellon, S. F. *J. Med. Chem.* **2008**, *51*, 2879.
- Boezio, A. A.; Berry, L.; Albrecht, B. K.; Bauer, D.; Bellon, S. F.; Bode, C. M.; Chen, A.; Choquette, D.; Dussault, I.; Hirai, S.; Kaplan-Lefko, P.; Larrow, J. F.; Lin, J.; Lohman, J.; Potashman, M. H.; Rex, K.; Santostefano, M.; Shah, K.; Shimanovich, R.; Springer, S. K.; Teffera, Y.; Yang, Y.; Zhang, Y.; Harmange, J.-C. *Bioorg. Med. Chem. Lett.* **2009**, *19*, 6307.
- The hydrogen bond framework in 3, between the proton at C-5 and the carbonyl, was not included for a clearer structural representation of the compound.
- Ishikawa, M.; Hashimoto, Y. *J. Med. Chem.* **2011**, *54*, 1539.
- Pierce, A. C.; Sandretto, K. L.; Bemis, G. W. *Proteins Struct. Funct. Gen.* **2002**, *49*, 567.
- Phenyl substitution at the C-6 position was tolerated, but not optimal, in the O- and N-linked series. The phenyl analog was synthesized first, based on synthetic precedent: Pinto, D. J. P.; Orwat, M. J.; Quan, M. L.; Han, Q.; Galemmo, R. A., Jr.; Amparo, E.; Wells, B.; Ellis, C.; He, M. Y.; Alexander, R. S.; Rossi, K. A.; Smallwood, A.; Wong, P. C.; Luetgen, J. M.; Rendina, A. R.; Knabb, R. M.; Mersinger, L.; Kettner, C.; Bai, S.; He, K.; Wexler, R. R.; Lam, P. Y. S. *Bioorg. Med. Chem. Lett.* **2006**, *16*, 4141.
- PDB deposition codes for the crystal structures of c-Met + 2 and c-Met + 3 are 4DEG and 4DEH, respectively.
- Albrecht, B. K.; Bellon, S.; Bode, C. M.; Boezio, A.; Choquette, D.; Harmange, J.-C. *PCT Int. Appl.* **2009**, 109, WO 2009143477.
- Ángyán, J. G.; Poirier, R. A.; Kucsman, Á.; Csizmadia, I. G. *J. Am. Chem. Soc.* **1987**, *109*, 2237.
- See Figure 3 for example of unsaturated core binding to c-Met.
- All solubility data reported as follows: 0.01 N HCl/PBS/SIF (μg/mL).
- See Figure 3 for determination of stereochemical preference and explanation for enantiomeric preference.
- Sulfur-containing heterocycles were the focus of our efforts due to the favorable S–O interaction described previously.
- Fluorinated aromatic substitutions were chosen based on their potencies in the N-linked triazolopyridazine series.
- PDB deposition code number for the crystal structure of c-Met + 23 is 4DEI.
- The absolute stereochemistry was assigned by crystallization of enantiopure 23 with unphosphorylated c-Met.

23. At a concentration of 1 μ M, compound **23** binds to c-Met (0.3 percent of control (POC)) and the following kinases: VEGFR2 (34 POC), KIT (26 POC) and PDGFRB (10 POC).
24. D'Angelo, N. D.; Bellon, S. F.; Booker, S. K.; Cheng, Y.; Coxon, A.; Dominguez, C.; Fellows, I.; Hoffman, D.; Hungate, R.; Kaplan-Lefko, P.; Lee, M. R.; Li, C.; Liu, L.; Rainbeau, E.; Reider, P. J.; Rex, K.; Siegmund, A.; Sun, Y.; Tasker, A. S.; Xi, N.; Xu, S.; Yang, Y.; Zhang, Y.; Burgess, T. L.; Dussault, I.; Kim, T-S. *J. Med. Chem.* **2008**, *51*, 5766.
25. The in vivo potency correlated well with the observed in vitro cellular IC₅₀ of 2 nM when corrected for observed free fraction in mouse plasma.
26. Data are mean \pm SD ($n = 3$). *P* values correspond to statistical difference between groups treated with vehicle + HGF and compound **23** by Oneway Anova followed by Bonferroni/Dunn post hoc test **p* < 0.0001.